SCIENCE CHINA
Life Sciences

•RESEARCH PAPER•

November 2022 Vol.65 No.11: 2205–2217
10.1007/s11427-022-2104-3

A 10-miRNA risk score-based prediction model for pathological complete response to neoadjuvant chemotherapy in hormone receptor-positive breast cancer

Chang Gong[1†], Ziliang Cheng[2†], Yaping Yang[1†], Jun Shen[2†], Yingying Zhu[3†], Li Ling[3,4†], Wanyi Lin[1], Zhigang Yu[5], Zhihua Li[6], Weige Tan[7], Chushan Zheng[2], Wenbo Zheng[7], Jiajie Zhong[8], Xiang Zhang[2], Yunjie Zeng[8], Qiang Liu[1], R. Stephanie Huang[9], Andrzej L. Komorowski[10], Eddy S. Yang[11], François Bertucci[12], Francesco Ricci[13], Armando Orlandi[14], Gianluca Franceschini[15], Kazuaki Takabe[16], Suzanne Klimberg[17], Naohiro Ishii[18], Angela Toss[19], Mona P. Tan[20], Mathew A Cherian[21] & Erwei Song[1*]

[1]*Guangdong Provincial Key Laboratory of Malignant Tumor Epigenetics and Gene Regulation, Guangdong-Hong Kong Joint Laboratory for RNA Medicine, Breast Tumor Center, Sun Yat-sen Memorial Hospital, Sun Yat-sen University, Guangzhou 510120, China;*
[2]*Department of Radiology, Sun Yat-sen Memorial Hospital, Sun Yat-sen University, Guangzhou 510120, China;*
[3]*Clinical Research Design Division, Clinical Research Center, Sun Yat-sen Memorial Hospital, Sun Yat-sen University, Guangzhou 510120, China;*
[4]*Department of Medical Statistics, School of Public Health, Sun Yat-sen University, Guangzhou 510080, China;*
[5]*Department of Breast Surgery, the Second Affiliated Hospital, Shandong University, Jinan 250033, China;*
[6]*Department of Breast Surgery, Key Laboratory of Breast Diseases, Third Hospital of Nanchang, Nanchang 330009, China;*
[7]*Department of Breast Surgery, the First Affiliated Hospital, Guangzhou Medical University, Guangzhou 510120, China;*
[8]*Department of Pathology, Sun Yat-sen Memorial Hospital, Sun Yat-sen University, Guangzhou 510120, China;*
[9]*Department of Experimental and Clinical Pharmacology, University of Minnesota, Minneapolis, MN 55455, USA;*
[10]*Department of Surgery, College of Medicine, University of Rzeszów, Rzeszów 35-959, Poland;*
[11]*Department of Radiation Oncology, O'Neal Comprehensive Cancer Center, University of Alabama at Birmingham School of Medicine, Birmingham, AL, USA;*
[12]*Laboratoty of Predictive Oncology, Institut Paoli-Calmettes, Centre de Recherche en Cancérologie de Marseille, INSERM UMR1068, CNRS UMR725, Marseille, France;*
[13]*Department of Drug Development and Innovation(D3i), Institut Curie, Paris 75005, France;*
[14]*Comprehensive Cancer Center, UOC di Oncologia Medica, Fondazione Policlinico Universitario A. Gemelli IRCCS, Rome 00168, Italy;*
[15]*Multidisciplinary Breast Unit, Fondazione Policlinico Universitario Agostino Gemelli IRCCS, Università Cattolica del Sacro Cuore, Rome 00168, Italy;*
[16]*Breast Surgery, Department of Surgical Oncology, Roswell Park Comprehensive Cancer Center, Buffalo, NY, USA;*
[17]*Department of Surgery, MD Anderson Cancer Center, Houston, TX 77030, USA;*
[18]*Department of Plastic and Reconstructive Surgery, International University of Health and Welfare Hospital, Nasushiobara City, Tochigi 329-2763, Japan;*
[19]*Department of Oncology and Hematology, University Hospital of Modena, Modena 41124, Italy;*
[20]*MammoCare: Breast Clinic and Surgery in Singapore, 228510, Singapore;*
[21]*The Ohio State University Comprehensive Cancer Center, Arthur G. James Cancer Hospital and Richard J. Solove Research Institute, Columbus, OH 43210, USA*

†Contributed equally to this work
*Corresponding authors (email: songew@mail.sysu.edu.cn)

Received January 12, 2022; accepted February 23, 2022; published online May 13, 2022

Patients with hormone receptor (HR)-positive tumors breast cancer usually experience a relatively low pathological complete response (pCR) to neoadjuvant chemotherapy (NAC). Here, we derived a 10-microRNA risk score (10-miRNA RS)-based model with better performance in the prediction of pCR and validated its relation with the disease-free survival (DFS) in 755 HR-positive breast cancer patients (273, 265, and 217 in the training, internal, and external validation sets, respectively). This model, presented as a nomogram, included four parameters: the 10-miRNA RS found in our previous study, progesterone receptor (PR), human epidermal growth factor receptor 2 (HER2) status, and volume transfer constant (K^{trans}). Favorable calibration and discrimination of 10-miRNA RS-based model with areas under the curve (AUC) of 0.865, 0.811, and 0.804 were shown in the training, internal, and external validation sets, respectively. Patients who have higher nomogram score (>92.2) with NAC treatment would have longer DFS (hazard ratio=0.57; 95%CI: 0.39–0.83; P=0.004). In summary, our data showed the 10-miRNA RS-based model could precisely identify more patients who can attain pCR to NAC, which may help clinicians formulate the personalized initial treatment strategy and consequently achieves better clinical prognosis for patients with HR-positive breast cancer.

hormone receptor-positive breast cancer, microRNA signature, neoadjuvant chemotherapy, dynamic contrast-enhanced magnetic resonance imaging, nomogram

Citation: Gong, C., Cheng, Z., Yang, Y., Shen, J., Zhu, Y., Ling, L., Lin, W., Yu, Z., Li, Z., Tan, W., et al. (2022). A 10-miRNA risk score-based prediction model for pathological complete response to neoadjuvant chemotherapy in hormone receptor-positive breast cancer. Sci China Life Sci 65, 2205–2217. 10.1007/s11427-022-2104-3

INTRODUCTION

Hormone receptor (HR)-positive tumors account for approximately 70% of all breast cancers, affecting more than 2 million patients each year (Kobayashi et al., 2017). Neoadjuvant chemotherapy (NAC) is the standard treatment for locally advanced HR-positive breast cancers and can contribute to the operability of locally advanced breast cancer (Fisher et al., 1997; Makris et al., 1998) and *in vivo* assessment sensitivity to systemic therapy (Asaoka et al., 2020; von Minckwitz et al., 2019). Pathological complete response (pCR) is mostly used to evaluate the degree of regression after NAC (Bear et al., 2003; Ferrière et al., 1998; Rastogi et al., 2008; von Minckwitz et al., 2012). Compared with those achieving non-pCR, patients with HR-positive breast cancer who attain pCR to NAC treatment usually experience improved survival (Cortazar et al., 2019; Yee et al., 2018). However, patients with HR-positive breast cancer usually experience a relatively low pCR to NAC treatment, ranging from 7% to 38% (Rouzier et al., 2005; von Minckwitz et al., 2011). Therefore, to identify those who can truly benefit from NAC by achieving pCR is imperative and can provide considerable clinical benefit in minimizing over- or under-treatment of NAC.

Thus far, a few clinicopathological factors (e.g., estrogen receptor (ER) status (Kasami et al., 2008), Ki-67 expression level (Vincent-Salomon et al., 2004), immunohistochemical 4-score (IHC4)) (Tan et al., 2016) and multigene classifiers (e.g., the Oncotype DX recurrence score (Pease et al., 2019), EndoPredict risk score (Dubsky et al., 2020), and PAM50 ProsignaROR Score (Prat et al., 2016)) have been used to predict the pCR to NAC in patients with breast cancer. However, the application of these prediction model in Asian countries has been limited due to their relatively low predictive ability, or without prospectively verify the relation of its score with clinical prognosis, or the small sample size or the small proportion of Asian participants included in these studies.

MicroRNAs (miRNAs), a class of endogenous 21–22 nt noncoding small RNAs, have shown their promise in the prognosis of breast cancer (Di Cosimo et al., 2019; Saw and Song, 2020). In our preliminary study, 10 miRNAs derived from the cancer tissue were found to have a better prognostic performance than both the IHC4 score and 21-gene recurrence score (areas under the curve (AUC): 0.710 *vs*. 0.602 *vs*. 0.685 respectively) (Gong et al., 2016). Besides, some studies with small sample sizes have reported the abilities of the kinetic parameters derived from dynamic contrast-enhanced magnetic resonance imaging (DCE-MRI), such as volume transfer constant (K^{trans}) or reverse reflux rate constant (K_{ep}) (AUC: 0.56–0.66) in predicting pCR to NAC treatment in patients with all subtypes of breast cancer (Drisis et al., 2016; Pickles et al., 2005). However, the ability of the 10-microRNA risk score (10-miRNA RS) or kinetic parameters from DCE-MRI in predicting the pCR to NAC before treatment has not been examined in patients with HR-positive breast cancer.

Thus, in this prospective study, we aimed to investigate (i) whether the 10-miRNA RS, kinetic parameters derived from DCE-MRI, alone or combination can predict pCR before NAC treatment, and (ii) whether the score of the established predictive model is related with the disease-free survival (DFS) of NAC-treated patients with HR-positive breast cancer. A prediction model with high accuracy for predicting

pCR to NAC and better clinical prognosis is desirable to facilitate personalized treatment decision-making by choosing NAC treatment or not for patients with HR-positive breast cancer.

RESULTS

Baseline clinicopathological status of the training and validation sets

The baseline characteristics of the 755 patients with median age 46 years (range 20–84 years) are shown in Table 1. The overall pCR rate was 17.1% (n=129), with 19.0% (52/273), 13.6% (36/265), and 18.9% (41/217) of patients in the training, internal and external validation cohort respectively. The mean (SD) of 10-miRNA RS in all patients was 2.69 (2.21), while the means in the training, internal and external validation cohort were 2.70 (2.24), 2.88 (2.18), and 2.46 (2.19) correspondingly. In all patients, there are 77.6% (586/755) patients with both anthracycline and paclitaxel, while 10.5% (79/755) and 8.9% (67/755) received NAC with paclitaxel or anthracycline separately. There are 288 (38.1%) patients with human epidermal growth factor receptor 2 (HER2) positive and receiving trastuzumab therapy, including 26 (9.0%) who extra received pertuzumab treatment.

Construction and validation of the 10-miRNA RS-based model

The boxplot and scatter plot of 10-miRNA RS show that the 10-miRNA RS was positively correlated with pCR status (P<0.001) (Figure S1A and B in Supporting Information). The comparisons of baseline characteristics between patients with different pCR status in the training cohort are displayed in Table S1 in Supporting Information. Compared with those with non-pCR, patients with pCR had higher 10-miRNA RS, but lower ER expression level, progesterone receptor (PR) expression level, HER2-positive status, K^{trans}, K_{ep}, and volume fraction of extravascular extracellular space (V_e) values (P<0.05). Representative DCE-MR images obtained prior to NAC in patients are shown in Figure S2A and B in Supporting Information.

In the training set, univariable logistic analyses showed that pCR status was associated with 10-miRNA RS, HER2 status, PR level, ER level, K^{trans}, K_{ep}, and V_e (Table S2 in Supporting Information). However, multivariable logistic analysis showed only 10-miRNA RS, HER2 status, PR level, and K^{trans} to be independent predictors of pCR (Table S2 in Supporting Information). Therefore, these 4 factors were integrated into a model, named as the 10-miRNA RS-based model, with the coefficients being calculated as follows: $Logit(P)=-3.999+1.022*HER2+0.901*PR+1.731*RS+2.279*K^{trans}$.

The C-index of the nomogram was 0.866 (95% confidence index (95%CI): 0.811–0.921) 0.811 (95%CI: 0.742–0.880) and 0.804 (95%CI: 0.734–0.880) in the training, internal and external validation sets, respectively. The calibration curves for the probability of attaining pCR in the training and validation cohorts are shown in Figure S3A–C in Supporting Information, and suggested good correlations between nomogram-predicted and observed pCR status. The 10-miRNA RS-based model was then configured as a nomogram for clinical use (Figure 1).

Comparisons with other models

The performance of the nomogram was compared with that of the 10-miRNA RS-alone model, the K^{trans}-alone model, and the IHC4 model in the training, internal and external validation sets separately. The AUC of the nomogram (0.865; 95%CI: 0.809–0.921) for predicting pCR was significantly higher than that of the 10-miRNA RS-alone model (0.720; 95%CI: 0.638–0.801; P=0.001), the K^{trans}-alone model (0.733; 95%CI: 0.645–0.820; P<0.001), and the IHC4 model (0.691; 95%CI: 0.619–0.763; P<0.001) in the training set. Similarly, in the internal validation cohort, the AUC of the nomogram (AUC=0.811; 95%CI: 0.724–0.880) for predicting pCR was significantly higher than that of the 10-miRNA RS-alone (AUC=0.668; 95%CI: 0.583–0.752; P=0.002), K^{trans}-alone (AUC=0.743, 95%CI: 0.650–0.835; P=0.049), and IHC4 (AUC=0.655, 95%CI: 0.568–0.744; P=0.001) model. In the external validation cohort, the nomogram had a significantly higher AUC (AUC=0.804; 95% CI: 0.734–0.873) than did the 10-miRNA RS-alone (AUC=0.736; 95%CI: 0.664–0.807; P=0.048), K^{trans}-alone (AUC=0.670; 95%CI: 0.571–0.768; P=0.004), or IHC4 (AUC=0.691; 95%CI: 0.608–0.774; P=0.015) model for the prediction of pCR. The details are shown in Figure 2A–C.

Among patients predicted accurately to attain pCR by the 10-miRNA RS-based model, only 80.9% (89/110) were detected by the IHC4 model. Patients with HER2-negative, and a high proportion of ER≥10% and PR≥20% could be identified to attain pCR after NAC treatment by the 10-miRNA RS-based model rather than the IHC4 model (Table 2).

Clinical utility of the nomogram

The decision curve analysis (DCA) for the nomogram, the 10-miRNA RS-alone, K^{trans}-alone, and IHC4 model demonstrated that the optimized model provided a higher net benefit for predicting pCR across a wider reasonable range (3%–88%) of threshold probabilities (Figure 3A).

The overall pCR scores of the 755 patients ranged from 0 to 260.3. The threshold of the maximal Youden index for pCR status was 92.2. The probability of achieving pCR was 12.80 (95%CI: 7.64–21.43) times higher in patients with a

Table 1 Characteristics of patients in training and validation sets[a)]

Characteristics	Training set *N*=273 (%)	Internal validation set *N*=265 (%)	External validation set *N*=217 (%)	Total *N*=755 (%)
pCR status				
Non-pCR	221 (81.0)	229 (86.4)	176 (81.1)	626 (82.9)
pCR	52 (19.0)	36 (13.6)	41 (18.9)	129 (17.1)
10-miRNA RS	2.70±2.24	2.88±2.18	2.46±2.19	2.69±2.21
K^{trans} (min^{-1})	0.19±0.10	0.20±0.12	0.21±0.12	0.20±0.12
K_{ep} (min^{-1})	1.14±0.54	1.19±0.64	1.19±0.67	1.17±0.61
V_e	0.17±0.07	0.16±0.07	0.17±0.08	0.17±0.07
V_p	0.02±0.03	0.03±0.12	0.04±0.11	0.03±0.10
ADC value ($\times10^{-3}mm^2\ s^{-1}$)	0.85±0.16	0.86±0.16	0.87±0.16	0.86±0.16
Morphology				
Mass	245 (89.7)	231 (87.2)	194 (89.4)	670 (88.7)
NME	28 (10.3)	34 (12.8)	23 (10.6)	85 (11.3)
Internal enhancement characteristics				
Homogeneous	80 (29.3)	49 (18.5)	55 (25.3)	184 (24.4)
Heterogeneous	163 (59.7)	182 (68.7)	139 (64.1)	484 (64.1)
Rim enhancement	30 (11.0)	34 (12.8)	23 (10.6)	87 (11.5)
TIC				
Persistent	16 (5.9)	21 (7.9)	15 (6.9)	52 (6.9)
Plateau	223 (81.7)	206 (77.7)	158 (72.8)	587 (77.7)
Washout	34 (12.5)	38 (14.3)	44 (20.3)	116 (15.4)
Age				
≤50	186 (68.1)	166 (62.6)	129 (59.4)	481 (63.7)
>50	87 (31.9)	99 (37.4)	88 (40.6)	274 (36.3)
Menopausal status				
Premenopausal	175 (64.1)	147 (55.5)	119 (54.8)	441 (58.4)
Postmenopausal	98 (35.9)	118 (44.5)	98 (45.2)	314 (41.6)
ER[*]				
Low	48 (17.6)	90 (34.0)	72 (33.2)	210 (27.8)
High	225 (82.4)	175 (66.0)	145 (66.8)	545 (72.2)
PR[#]				
Low	121 (44.3)	103 (38.9)	85 (39.2)	340 (45.0)
High	152 (55.7)	162 (61.1)	132 (60.8)	415 (55.0)
HER2[**]				
Negative	181 (66.3)	163 (61.5)	123 (56.7)	467 (61.9)
Positive	92 (33.7)	102 (38.5)	94 (43.3)	288 (38.1)
Ki-67[##]				
Negative	16 (5.9)	13 (4.9)	18 (8.3)	47 (6.2)
Positive	257 (94.1)	252 (95.1)	199 (91.7)	708 (93.8)
Tumor size[@]				
≤5 cm	214 (78.4)	207 (78.1)	153 (70.5)	574 (76.0)
>5 cm	59 (21.6)	58 (21.9)	64 (29.5)	181 (24.0)
cN stage[&]				
N0-1	208 (76.2)	218 (82.3)	170 (78.3)	596 (78.9)
N2-3	65 (23.8)	47 (17.7)	47 (21.7)	159 (21.1)

(*To be continued on the next page*)

(*Continued*)

Characteristics	Training set *N*=273 (%)	Internal validation set *N*=265 (%)	External validation set *N*=217 (%)	Total *N*=755 (%)
Grade				
II	121 (44.3)	128 (48.3)	99 (45.6)	348 (46.1)
III	101 (37.0)	79 (29.8)	60 (27.6)	240 (31.8)
Unknown	51 (18.7)	58 (21.9)	58 (26.7)	167 (22.1)
Pathologic type				
IDC	263 (96.3)	258 (97.4)	205 (94.5)	726 (96.2)
ILC	6 (2.2)	5 (1.9)	6 (2.8)	17 (2.3)
Other	4 (1.5)	2 (0.8)	6 (2.8)	12 (1.6)
Surgery				
Mastectomy	177 (64.8)	181 (68.3)	154 (71.0)	512 (67.8)
BCS	96 (35.2)	84 (31.7)	63 (29.0)	243 (32.2)
Axillary surgery				
SLNB	54 (19.8)	55 (20.8)	35 (16.1)	144 (19.1)
ALND	219 (80.2)	210 (79.2)	182 (83.9)	611 (80.9)
NAC				
Anthracycline and paclitaxel-based	221 (81.0)	202 (76.2)	163 (75.1)	586 (77.6)
Paclitaxel-based	25 (9.2)	30 (11.3)	24 (11.1)	79 (10.5)
Anthracycline-based	25 (9.2)	26 (9.8)	14 (6.5)	67 (8.9)
Other regiments[$]	2 (0.7)	7 (2.6)	16 (7.4)	23 (3.0)
Endocrine therapy				
Aromatase inhibitor	162 (59.3)	149 (56.2)	129 (59.4)	440 (58.3)
Tamoxifen	111 (40.7)	116 (43.8)	88 (40.6)	315 (41.7)
HER2-positive therapy				
Trastuzumab	86 (93.5)	93 (91.2)	83 (88.3)	262 (91.0)
Trastuzumab+pertuzumab	6 (6.5)	9 (8.8)	11 (11.7)	26 (9.0)
Radiation therapy				
No	70 (25.6)	87 (32.8)	93 (42.9)	250 (33.1)
Yes	203 (74.4)	178 (67.2)	124 (57.1)	505 (66.9)

a) Abbreviations: PR, progesterone receptor; IDC, invasive ductal carcinoma; ILC, invasive lobular carcinoma; BCS, breast conserving surgery; SLNB, sentinel lymph node biopsy; ALND, axillary lymph node dissection; V_e, volume fraction of extravascular extracellular space; V_p, volume fraction of plasma; NME, non-mass enhancement; ADC, apparent diffusion coefficient; TIC, time-signal intensity curve. *, Cases where ≥10% of tumor cells stained positive for ER with immunohistochemistry (IHC) were considered high. #, Cases where ≥20% of tumor cells stained positive for PR with IHC were considered high. **, Cases that showed either 3+ IHC staining or had gene copy number>2.0 were considered HER2 positive. ##, Cases where ≥14% of tumor cells stained positive for Ki-67 with IHC were considered positive. @, The maximum diameter measured at the 90 s of DCE-MRI. &, Nobal staging performed by means of palpation and US without biopsy confirmation. $, Either with single-agent anthracycline, vinorelbine or combined with platinum, etc.

score >92.2 than in patients with a score ≤92.2 (P<0.001). Of the 755 patients in this study, 18.7% (141/755) progressed to local or regional recurrence, distant metastasis, contralateral breast cancer, or death. The median length of follow-up was 29 months (range 4–108 months). The Kaplan-Meier survival curve for the nomogram score with DFS is presented in Figure 3B. Multivariable Cox proportional regression revealed that compared with those with a score≤92.2, patients with a score>92.2 were more likely to have longer DFS (hazard ratio (HR)=0.57; 95%CI: 0.39–0.83; P=0.004), even after adjustment for ER expression level and tumor size (Table 3).

DISCUSSION

In this multicenter study, we developed and validated a 10-miRNA RS-based model presented as a nomogram and achieved a high predictive performance for pCR to NAC in patients with HR-positive breast cancer. The performance of 10-miRNA RS-based model was significantly better than that of the IHC4 prediction model, especially for high HR-positive (ER≥10%, PR≥20%) and HER2-negative patients. Compared with those with a low nomogram score (≤92.2), patients with a high nomogram score (>92.2) were more likely to have longer DFS .

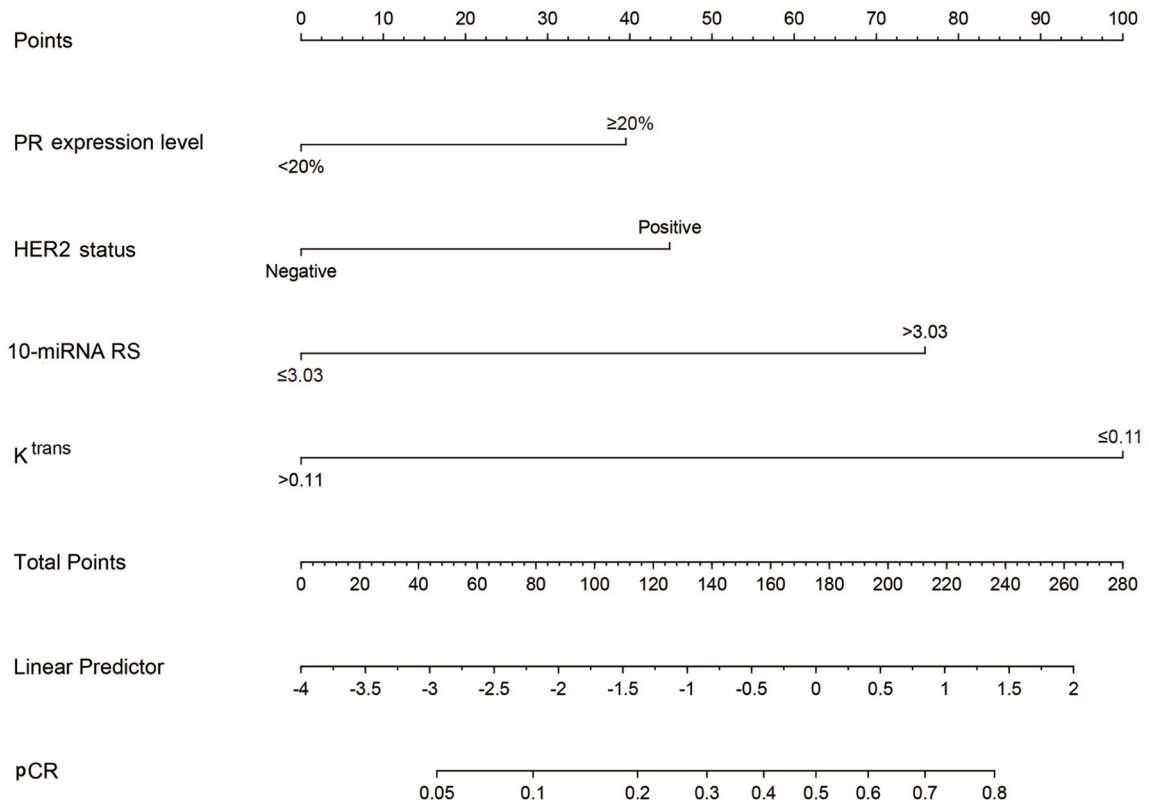

Figure 1 Nomogram to predict pCR probability for patients with HR-positive breast cancer. A nomogram incorporating 10-miRNA RS score, K^{trans}, HER2 status, and PR status was developed using the training cohort and was validated in the validation cohort. The sum of the scores is located on the Total Points axis. Based on the total score, the probability of pCR for patients with HR-positive breast cancer can be predicted.

One of the most important issues in the treatment of luminal early breast cancer is determining which patients can receive maximum benefit from chemotherapy. However, patients with luminal subtypes of breast cancer benefit differently from chemotherapy. Tumors with elevated HR level exhibit increased responsiveness to endocrine therapy (Chen et al., 2018). In the neoadjuvant setting for luminal-like tumors, identifying those patients who can truly benefit from NAC is crucial for successfully sparing toxicity and optimally selecting patients for endocrine or targeted therapy versus chemotherapy. It should be noted that all predictors was collected before initial treatment in our study. The established 10-miRNA RS-based model achieved a higher predictive performance for pCR to NAC. Meanwhile, compared with IHC4 model, the integrated model could identify more patients with HER negative, and high ER and PR who can attain pCR after NAC treatment. Patients with high model score would have better clinical prognosis after NAC treatment. By using this scoring system, patients with different probabilities of pCR to NAC can be identified before the initiation of NAC, which may have significant clinical value in guiding the preoperative decision-making for HR-positive patients, especially those with ER≥10%, PR≥20% and HER2-negative patients.

The prognostic ability of several multiple gene classifiers, such as the 21-gene assay (Sparano et al., 2021), the 70-gene MammaPrint signature (Whitworth et al., 2014), the PAM50 (Prat et al., 2016), and EPclin (Filipits et al., 2011), has already been verified. However, current multigene classifiers cannot yet be routinely recommended for the prediction of pCR owing to the small-sample-size clinical trials and relatively low predictive abilities on HR-positive patients. The heterogeneity of the HR-positive breast cancers may not be adequately characterized by conventional multigene assays that do not consider underlying aggressive non-luminal gene expression profiles.

Noticeably, the 10-miRNAs incorporated into our predictive model regulate diverse biological characteristics and processes of breast cancer cells, such as stem cell-like properties (Yu et al., 2010), chemotherapeutic sensitivity (Han et al., 2019), apoptosis (Yu et al., 2010), and metastasis (Chen et al., 2015), via targeting multiple genes. It is reasonable to assume that the combination of these miRNAs may render a more comprehensive model for predicting chemotherapeutic response of breast cancer than that derived from previously devised genetic signatures, which have mostly involved proliferation-related genes (Reis-Filho and Pusztai, 2011; Saw et al., 2021). It should be noted that 3 of the incorporated miRNAs (miR-21, miR-125b, and miR-200c) play a critical role in regulating the proliferation and

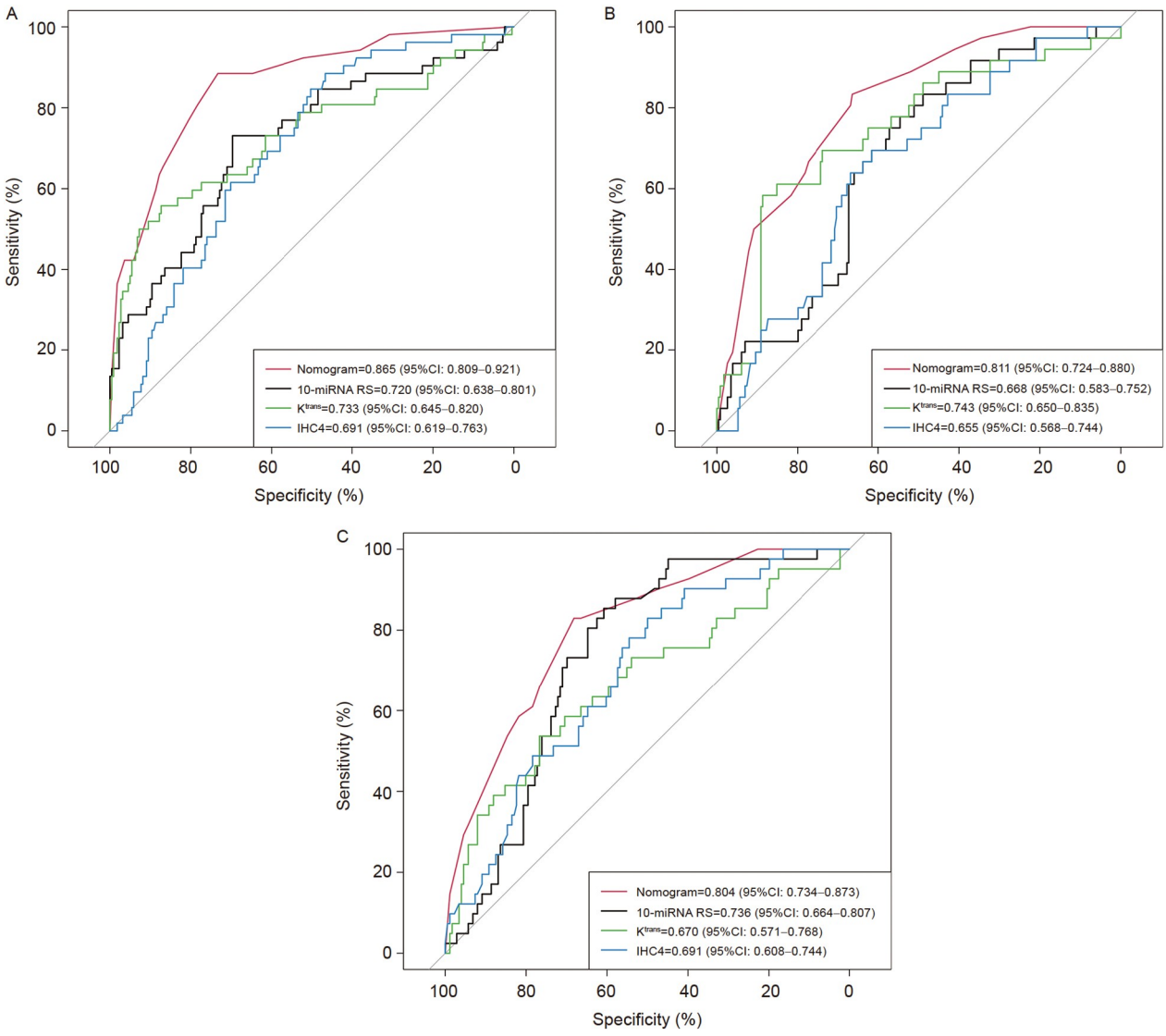

Figure 2 Discriminatory accuracy for predicting pCR status as assessed by ROC analysis to calculate the AUC. The training cohort (A), the internal validation cohort (B), and the external validation cohort (C). ROC, receiver operating characteristic curve; model, the nomogram model.

drug resistance of cells in HER2-positive breast cancer (Gong et al., 2011; Kutanzi et al., 2011; Tang et al., 2019). Compared with nonresponders, NAC responders show significantly lower levels of miR-21 (McGuire et al., 2020); furthermore, low intratumoral expression of miR-7 prior to NAC can identify those patients unlikely to achieve pCR (Raychaudhuri et al., 2017).

Tumor cells appear to be more resistant to chemotherapy due to the increased leakage space and intravascular blood volume (Jain, 2005; Kim et al., 2017; Viallard and Larrivée, 2017; Zhao et al., 2020). Kinetic parameters can reflect tumor angiogenesis in a noninvasive and quantitative manner. The underlying pathological abnormalities of tumor angiogenesis can lead to an increase in K^{trans} (Cheng et al., 2018), and higher K^{trans} has also been identified as an indicator of poor prognosis in breast cancer (Koo et al., 2012). Makris et al. (1999) reported fewer tumor microvessels being found in patients with breast cancer who received chemotherapy than in untreated patients. In our study, a strong correlation was found between pre-treatemnt K^{trans} and pCR in both the training and validation sets. These findings suggest that basal K^{trans} could be an imaging biomarker for the early prediction of pCR to NAC treatment.

As mentioned above, most of the miRNAs incorporated into our 10-miRNA RS-based classifier play vital roles in regulating the function and progression of tumor cells (Chen et al., 2015; Han et al., 2019; Iorio et al., 2005; Yu et al., 2010). Moreover, kinetic parameters derived from DCE-MRI can reflect microvascular characteristics of cancer tissues (Li et al., 2015; Yi et al., 2014). In our study, the performance of this integrated model for predicting pCR to NAC was significantly higher than that of the 10-miRNA RS-alone, K^{trans}-alone, and IHC4 model. Thus, the combination of miRNA signatures, K^{trans}, and clinical-pathological

Table 2 The comparisons of clinical information according to the pCR status identified by IHC4 model in patients achieving pCR predicted by 10-miRNA RS-based model[a)]

Characteristics	non-pCR by IHC4 *N*=21 (%)	pCR by IHC4 *N*=89 (%)	*P* value
Age			0.678
≤50	14 (66.7)	55 (61.8)	
>50	7 (33.3)	34 (38.2)	
ER*			<0.001
Low	0 (0.0)	54 (60.7)	
High	21 (100.0)	35 (39.3)	
PR#			<0.001
Low	8 (38.1)	80 (89.9)	
High	13 (61.9)	9 (10.1)	
HER2**			0.001
Negative	15 (71.4)	28 (31.5)	
Positive	6 (28.6)	61 (68.5)	
Ki-67##			0.958
Negative	1 (4.8)	4 (4.5)	
Positive	20 (95.2)	85 (95.5)	
Tumor size			0.154
≤5 cm	19 (90.5)	67 (75.3)	
>5 cm	2 (9.5)	22 (24.7)	
cN stage			0.403
N0-1	18 (85.7)	66 (74.2)	
N2-3	3 (14.3)	23 (25.8)	
Grade			0.003
II	9 (42.9)	27 (30.3)	
III	10 (47.6)	19 (21.3)	
Unknown	2 (9.5)	43 (48.3)	
Pathologic type			0.242
IDC	19 (90.5)	86 (96.6)	
ILC	1 (4.8)	2 (2.2)	
Other	1 (4.8)	1 (1.1)	

a) Abbreviations: IDC, invasive ductal carcinoma; ILC, invasive lobular carcinoma. *, Cases where ≥10% of tumor cells stained positive for ER with immunohistochemistry (IHC) were considered high. #, Cases where ≥20% of tumor cells stained positive for PR with IHC were considered high. **, Cases that showed either 3+ IHC staining or had gene copy number>2.0 were considered HER2 positive. ##, Cases where ≥14% of tumor cells stained positive for Ki-67 with IHC were considered positive. *P* values of the comparison between 2 cohorts were generated by χ^2 test for categorical variables.

characteristics would provide valuable information about the biology of tumor, which may be highly associated with the sensitivity of NAC in HR-positive breast cancer.

In this study, we have shown how a multiparametric model based on molecular and imaging characteristics can be a more adequate predictive model in a disease as heterogeneous as locally advanced luminal breast cancer. However, our study still has several limitations. Firstly, although the composition of the patients was similar to that of other studies conducted during the same period (Killelea et al., 2015; Murphy et al., 2018), our relatively large prospective study contained few HR/HER2-positive patients treated with dual anti-HER2 monoclonal antibodies, reducing the precision of our estimates for these patients, which should be investigated in future studies. Secondly, head-to-head comparisons between the 10-miRNA RS-based model and other multigene classifiers, such as the PAM50, and EPclin, have not been conducted in this study. A series of head-to-head clinical trials should be initiated in the future.

In summary, we developed an integrative 10-miRNA RS-based model for predicting pCR to NAC in patients with HR-positive breast cancer. As the performance in predicting pCR was good and its relation with better survival, the constructed nomogram may facilitate personalized treatment decision-making and consequently improve the clinical prognosis for patients with HR-positive breast cancer.

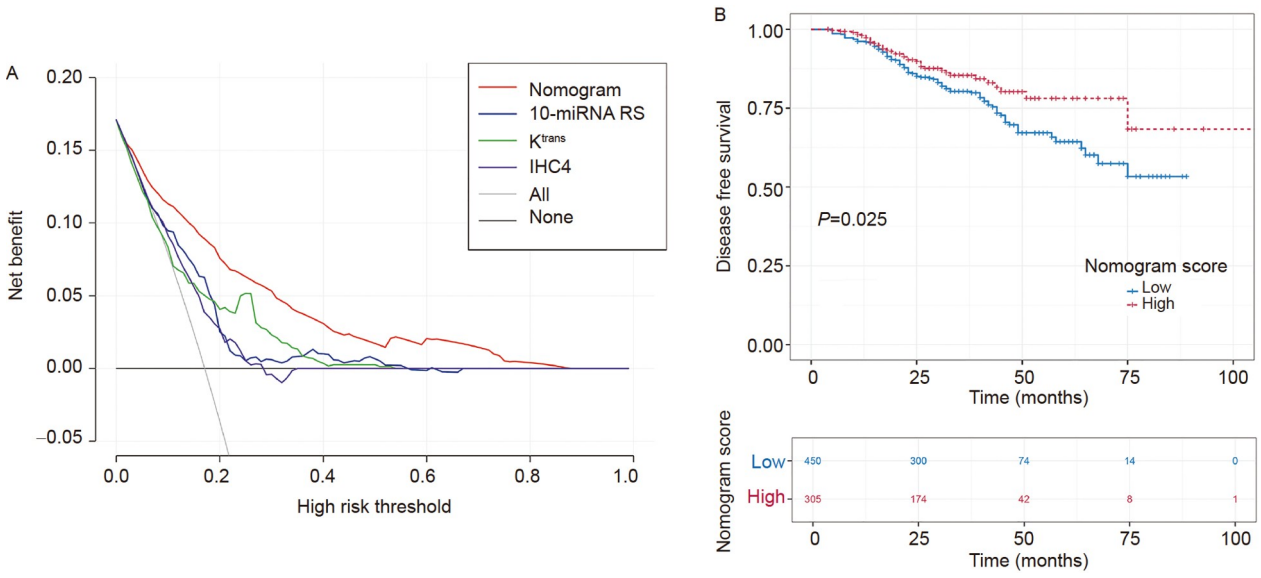

Figure 3 The DCA of the 4 predictors and the optimized model (A) and disease-free survival curves for all patients according to the nomogram score groups (B). The vertical axis represents the value of net benefit, and the horizontal axis shows the clinical usefulness of each model based on a continuum of potential thresholds for pCR probability. The preferred model is the 10-miRNA RS-based optimized model; it has the highest net benefit across a wider reasonable range (3%–88%) of threshold probabilities for predicting pCR compared with the use of the 10-miRNA RS, K^{trans}, or IHC4 alone.

Table 3 Univariable and Multivariable COX regression of variables with DFS in all patients[a)]

Variable	Univariate (*N*=755)		Multivariate (*N*=755)	
	Hazard ratio (95%CI)	*P*	Hazard ratio (95%CI)	*P*
pCR satus (pCR *vs*. non-pCR)	0.50 (0.28–0.88)	0.016	–	
Age (>50 *vs*. ≤50)	1.05 (1.14–4.67)	0.771	–	
Menopausal status (Post *vs*. Pre)	0.94 (0.46–1.93)	0.861	–	
ER* (low *vs*. high)	1.50 (1.05–2.14)	0.027	1.65 (1.13–2.41)	0.009
PR# (low *vs*. high)	1.40 (1.00–1.96)	0.052	–	
HER2** (positive *vs*. negative)	0.84 (0.60–1.20)	0.337	–	
Ki-67 (positive *vs*. negative)	0.82 (0.43–1.55)	0.536	–	
Tumor size (>5 cm *vs*. ≤5 cm)	2.32 (1.64–3.27)	<0.001	2.23 (1.57–3.15)	<0.001
cN (N2-3 *vs*. N0-1)	1.32 (0.91–1.92)	0.144	–	
Grade (III *vs*. II)	1.51 (1.04–2.19)	0.03	–	
Surgery (Mastectomy *vs*. BCS)	1.51 (1.02–2.25)	0.04	–	
Axillary surgery (SLNB *vs*. ALND)	1.65 (0.99–2.74)	0.053	–	
Endocrine therapy (AI *vs*. TAM)	0.99 (0.71–1.38)	0.941	–	
HER2-positive therapy (HP *vs*. H)	1.26 (0.38–4.16)	0.7	–	
Radiation therapy (Yes *vs*. No)	1.15 (0.81–1.63)	0.445	–	
10-miRNA RS (>3.03 *vs*. ≤3.03)	0.52 (0.35–0.77)	0.001	–	
K^{trans} (≤0.11 *vs*. >0.11)	0.79 (0.50–1.26)	0.323	–	
K_{ep} (≤0.78 *vs*. >0.78)	0.90 (0.61–1.33)	0.596	–	
V_e (≤0.12 *vs*. >0.12)	1.37 (0.96–1.95)	0.085	–	
Nomogram score (>92.2 *vs*. ≤92.2)	0.66 (0.46–0.95)	0.026	0.57 (0.39–0.83)	0.004

a) Abbreviations: BCS, breast conserving surgery; SLNB, sentinel lymph node biopsy; ALND, axillary lymph node dissection; AI, aromatase inhibitor; TAM, tamoxifen; HP, trastuzumab+pertuzumab; H, trastuzumab. *, Cases where ≥10% of tumor cells stained positive for ER with immunohistochemistry (IHC) were considered high. #, Cases where ≥20% of tumor cells stained positive for PR with IHC were considered high. **, Cases that showed either 3+ IHC staining or had gene copy number>2.0 were considered HER2 positive.

PATIENTS AND METHODS

Study design and data sets

We used the prospectively collected data from an ongoing clinical trial (NCT01503905; ClinicalTrials.gov) and a multicenter prospective cohort (ChiCTR-DDD-17013651; chictr.org.cn) conducted in China between March 1, 2012 and April 30, 2020, which totally includes 870 female patients with HR-positive breast cancer who were scheduled to receive standard NAC according to the National Comprehensive Cancer Network (NCCN) guidelines. Totally, 115 patients were excluded due to a lack of standard treatment, or breast cancer samples. Finally, 755 female patients were included in this study. The details of the patient eligibility criteria are shown in Table S3 in Supporting Information.

Among 755 patients, 538 patients were recruited from Sun Yat-sen Memorial Hospital, and divided randomly (1:1) into the training set (273 patients) and the internal validation set (265 patients). External validation set included 217 patients from 3 other hospitals (the Second Affiliated Hospital of Shandong University, n=125; the Third Hospital of Nanchang City, n=60; and the First Affiliated Hospital of Guangzhou Medical University, n=32). The flow chart of the enrollment is shown in Figure 4. Ethical approval for this project was obtained from each participating hospital, and written informed consent was obtained from all patients.

Outcomes

The endpoint for developing the prediction model was the pCR rate after NAC treatment. According to the American Food and Drug Administration criteria (US Department of Health and Human Services Food and Drug Administration: https://www.fda.gov/regulatory-information/search-fda-guidance-documents/pathological-complete-response-neoadjuvant-treatment-high-risk-early-stage-breast-cancer-use), pCR (ypT0/Tis-ypN0) is defined as the absence of residual invasive tumor in the breast and axillary lymph nodes on the operative specimen (breast tumor and axillary lymph nodes) after standard NAC treatment. Another endpoint used to estimate the clinical value of the prediction model was DFS, which was defined as the time from tumor surgery after NAC to local or regional recurrence, distant metastasis, contralateral breast cancer, death, or the last follow-up visit.

Data collection of predictors

Our candidate predictors included clinical information, clinicpathological features, 10 miRNA-RS, and MRI parameters. Required clinical information included such as patients' age, tumor-node-metastasis (TNM) stage, and the types of adjuvant therapies. Primary breast cancer samples obtained before the treatment of NAC by core needle biopsy were used to assess the clinicopathological features, for example ER, PR, and HER2 expression according to the World Health Organization (WHO) classification of breast tumors (Board, 2019).

The related miRNAs were quantified in the samples of breast cancer collected before NAC treatment. The 10 miRNAs were miR-30c, miR-21, miR-181a, miR-181c, miR-125b, miR-7, miR-200a, miR-135b, miR-22, and miR-200c, which were detected by the method described in a previous study (Gong et al., 2016). The details of measurement of 10 miRNAs were described in Supplementary Methods and Table S4 in Supporting Information. The 10-miRNA RS was calculated according to this previously established and validated formula:

$$\begin{aligned}\text{10-miRNA RS} = {} & 0.165*\lg^{\text{miR-21}} - 0.812*\lg^{\text{miR-30c}} \\ & +1.053*\lg^{\text{miR-181a}} + 0.179*\lg^{\text{miR-181c}} \\ & +0.672*\lg^{\text{miR-125b}} - 0.588*\lg^{\text{miR-7}} \\ & -0.469*\lg^{\text{miR-200a}} + 1.065*\lg^{\text{miR-135b}} \\ & -0.986*\lg^{\text{miR-22}} - 0.820*\lg^{\text{miR-200c}}.\end{aligned}$$

Breast MRI was underwent before biopsy and within 1 week before NAC. MRI parameters such as kinetic parameters (K^{trans}, K_{ep}, V_e, and volume fraction of plasma (V_p)), apparent diffusion coefficient (ADC) values, and type of time-signal intensity curve (TIC) were analysed.

The details about the examination and quantification of 10 miRNAs and MRI parameters are provided in the Supplementary Methods and Table S5 in Supporting Information.

Statistical analysis

In this study, the 10-miRNA RS and the values of kinetic parameters were divided into binary variables according to the threshold determined by the maximal Youden index of pCR status, in which the highest predictive value of pCR is shown. Descriptive statistics for all patients and three different sets separately were reported as mean and standard deviation (SD) for continuous variables, and frequencies and percentages for categorical variables. In the training set, the distribution of the 10-miRNA RS with pCR status after NAC treatment was analysed by scatter diagram and boxplot. The between-group difference in patients with pCR and those without pCR were examined by t-tests or χ^2 test. The significant variables were then identified with univariable logistic regression analyses and included in multivariable logistic regression analyses via forward conditional selection to establish the predictive model. The predictive model was finally named as the 10-miRNA RS-based model and presented as a nomogram. The discrimination and calibration of the nomogram was determined by using the Harrell's concordance index (C-index) and calibration curves.

The performance of the nomogram was also evaluated by

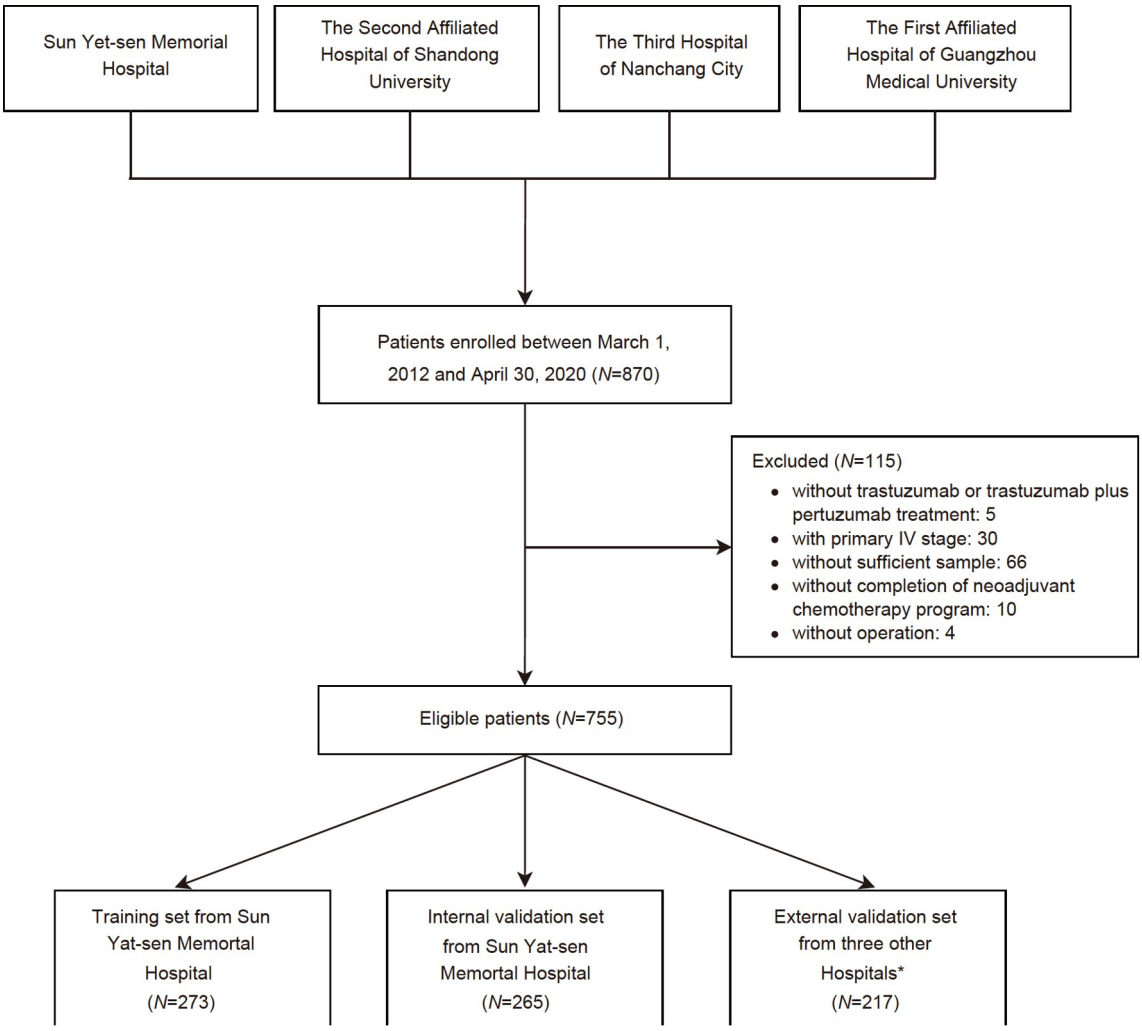

Figure 4 Flowchart of enrollment in the study. A total of 755 patients were enrolled in the study. From Sun Yat-sen Memorial Hospital, 273 patients were enrolled as the training cohort, and 265 patients were used as the internal validation cohort.*, For the external validation cohort, 217 patients were enrolled from 3 other centers: the Second Affiliated Hospital of Shandong University (n=125), the Third Hospital of Nanchang City (n=60), and the First Affiliated Hospital of Guangzhou Medical University (n=32).

comparing the area under the receiver operating characteristic curve (AUC) with that of the 10-miRNA RS-alone model, the K^{trans}-alone model, and IHC4 model separately. The calculation of the IHC4 algorithm was performed according to a previous article (Cuzick et al., 2011). In order to identify the inconsistency, the characteristics of patients achieving pCR predicted by the 10-miRNA RS-based model were compared according to the pCR status (pCR *vs*. non-pCR) predicted by the IHC4 model in the training set.

For clinical utility, the DCA for the 4 clinical prediction models (the 10-miRNA RS-based, 10-miRNA RS-alone, K^{trans}-alone, and IHC4 model) was used to calculate the net benefits for a range of threshold probabilities (Vickers et al., 2008). Moreover, univariable and multivariable Cox proportional regression with forward conditional selection was used to verify the association between predicted nomogram score and DFS after NAC treatment in all patients. Survival curves were estimated using the Kaplan-Meier method. The predicted nomogram scores were put into analysis as a binary variable (high *vs*. low) divided by the threshold where the maximal Youden index of pCR status existed.

Two-sided P values less than 0.05 were considered to be statistically significant. All statistical analyses were performed using R software (version 3.6.3). The code for analyses were shown in Supplementary Methods.

Data sharing

The individual participant data will be shared to a study proposal approved by an accredited ethics committee. Methodologically sound proposals for any purpose will be considered by the study committee. Proposals should be made by email to the corresponding author. To gain access, data requester will need to sign a data access agreement.

Compliance and ethics *The author(s) declare that they have no conflict of interest. Presented in poster format at the 55th Annual Meeting of the American Society of Clinical Oncology, Chicago, IL, May 31 to June 4, 2019.*

Acknowledgements *This work was supported by the National Natural Science Foundation of China (92159303, 81621004, 81720108029, 81930081, 91940305, 81672594, 81772836, 81872139, 82072907, and 82003311), Guangdong Science and Technology Department (2020B1212060018 and 2020B1212030004), Clinical Innovation Research Program of Bioland Laboratory (2018GZR0201004), Bureau of Science and Technology of Guangzhou (20212200003), Program for Guangdong Introducing Innovative and Enterpreneurial Teams (2019BT02Y198), the Project of The Beijing Xisike Clinical Oncology Research Foundation (Y-Roche2019/2-0078), the Technology Development Program of Guangdong province (2021A0505030082), the Project of The Guangdong Provincial Key Laboratory of Malignant Tumor Epigenetics and Gene Regulation (2020B1212060018), Sun Yat-Sen Memorial Hospital Cultivation Project for Clinical Research (SYS-C-201805 and SYS-Q-202004), Guangzhou Science and Technology Program (202102010272), and Medical Science and Technology Research Fund of Guangdong Province (A2020391). The authors appreciate the academic support from the AME Breast Cancer Collaborative Group and Claire Verschraegen for her critical review of the manuscript.*

References

Asaoka, M., Gandhi, S., Ishikawa, T., and Takabe, K. (2020). Neoadjuvant chemotherapy for breast cancer: past, present, and future. Breast Cancer 14, 117822342098037.

Bear, H.D., Anderson, S., Brown, A., Smith, R., Mamounas, E.P., Fisher, B., Margolese, R., Theoret, H., Soran, A., Wickerham, D.L., et al. (2003). The effect on tumor response of adding sequential preoperative docetaxel to preoperative doxorubicin and cyclophosphamide: preliminary results from national surgical adjuvant breast and bowel project protocol B-27. J Clin Oncol 21, 4165–4174.

Board, W.C.O.T.E. (2019). Breast Tumors. Lyon (France): International Agency for Research on Cancer. Available from URL: https://publications.iarc.fr/581.

Chen, B., Tang, H., Liu, X., Liu, P., Yang, L., Xie, X., Ye, F., Song, C., Xie, X., and Wei, W. (2015). MiR-22 as a prognostic factor targets glucose transporter protein type 1 in breast cancer. Cancer Lett 356, 410–417.

Chen, T., Zhang, N., Moran, M.S., Su, P., Haffty, B.G., and Yang, Q. (2018). Borderline ER-positive primary breast cancer gains no significant survival benefit from endocrine therapy: a systematic review and meta-analysis. Clin Breast Cancer 18, 1–8.

Cheng, Z., Wu, Z., Shi, G., Yi, Z., Xie, M., Zeng, W., Song, C., Zheng, C., and Shen, J. (2018). Discrimination between benign and malignant breast lesions using volumetric quantitative dynamic contrast-enhanced mr imaging. Eur Radiol 28, 982–991.

Cortazar, P., Zhang, L., Untch, M., Mehta, K., Costantino, J.P., Wolmark, N., Bonnefoi, H., Cameron, D., Gianni, L., Valagussa, P., et al. (2019). Pathological complete response and long-term clinical benefit in breast cancer: The ctneobc pooled analysis (vol 384, pg 164, 2014). Lancet 393, 986.

Cuzick, J., Dowsett, M., Pineda, S., Wale, C., Salter, J., Quinn, E., Zabaglo, L., Mallon, E., Green, A.R., Ellis, I.O., et al. (2011). Prognostic value of a combined estrogen receptor, progesterone receptor, Ki-67, and human epidermal growth factor receptor 2 immunohistochemical score and comparison with the genomic health recurrence score in early breast cancer. J Clin Oncol 29, 4273–4278.

Di Cosimo, S., Appierto, V., Pizzamiglio, S., Tiberio, P., Iorio, M.V., Hilbers, F., de Azambuja, E., de la Peña, L., Izquierdo, M., Huober, J., et al. (2019). Plasma miRNA levels for predicting therapeutic response to neoadjuvant treatment in HER2-positive breast cancer: results from the NeoALTTO trial. Clin Cancer Res 25, 3887–3895.

Drisis, S., Metens, T., Ignatiadis, M., Stathopoulos, K., Chao, S.L., and Lemort, M. (2016). Quantitative DCE-MRI for prediction of pathological complete response following neoadjuvant treatment for locally advanced breast cancer: The impact of breast cancer subtypes on the diagnostic accuracy. Eur Radiol 26, 1474–1484.

Dubsky, P.C., Singer, C.F., Egle, D., Wette, V., Petru, E., Balic, M., Pichler, A., Greil, R., Petzer, A.L., Bago-Horvath, Z., et al. (2020). The endopredict score predicts response to neoadjuvant chemotherapy and neoendocrine therapy in hormone receptor-positive, human epidermal growth factor receptor 2-negative breast cancer patients from the ABCSG-34 trial. Eur J Cancer 134, 99–106.

Ferrière, J.P., Assier, I., Curé, H., Charrier, S., Kwiatkowski, F., Achard, J. L., Dauplat, J., and Chollet, P. (1998). Primary chemotherapy in breast cancer. Am J Clin Oncol 21, 117–120.

Filipits, M., Rudas, M., Jakesz, R., Dubsky, P., Fitzal, F., Singer, C.F., Dietze, O., Greil, R., Jelen, A., Sevelda, P., et al. (2011). A new molecular predictor of distant recurrence in ER-positive, HER2-negative breast cancer adds independent information to conventional clinical risk factors. Clin Cancer Res 17, 6012–6020.

Fisher, B., Brown, A., Mamounas, E., Wieand, S., Robidoux, A., Margolese, R.G., Cruz Jr, A.B., Fisher, E.R., Wickerham, D.L., Wolmark, N., et al. (1997). Effect of preoperative chemotherapy on local-regional disease in women with operable breast cancer: findings from national surgical adjuvant breast and bowel project B-18. J Clin Oncol 15, 2483–2493.

Gong, C., Yao, Y., Wang, Y., Liu, B., Wu, W., Chen, J., Su, F., Yao, H., and Song, E. (2011). Up-regulation of miR-21 mediates resistance to trastuzumab therapy for breast cancer. J Biol Chem 286, 19127–19137.

Gong, C., Tan, W., Chen, K., You, N., Zhu, S., Liang, G., Xie, X., Li, Q., Zeng, Y., Ouyang, N., et al. (2016). Prognostic value of a BCSC-associated microRNA signature in hormone receptor-positive HER2-negative breast cancer. Ebiomedicine 11, 199–209.

Han, B., Huang, J., Han, Y., Hao, J., Wu, X., Song, H., Chen, X., Shen, Q., Dong, X., Pang, H., et al. (2019). The microRNA miR-181c enhances chemosensitivity and reduces chemoresistance in breast cancer cells via down-regulating osteopontin. Int J Biol Macromol 125, 544–556.

Iorio, M.V., Ferracin, M., Liu, C.G., Veronese, A., Spizzo, R., Sabbioni, S., Magri, E., Pedriali, M., Fabbri, M., Campiglio, M., et al. (2005). MicroRNA gene expression deregulation in human breast cancer. Cancer Res 65, 7065–7070.

Jain, R.K. (2005). Normalization of tumor vasculature: an emerging concept in antiangiogenic therapy. Science 307, 58–62.

Kasami, M., Uematsu, T., Honda, M., Yabuzaki, T., Sanuki, J., Uchida, Y., and Sugimura, H. (2008). Comparison of estrogen receptor, progesterone receptor and HER-2 status in breast cancer pre- and post-neoadjuvant chemotherapy. Breast 17, 523–527.

Killelea, B.K., Yang, V.Q., Wang, S.Y., Hayse, B., Mougalian, S., Horowitz, N.R., Chagpar, A.B., Pusztai, L., and Lannin, D.R. (2015). Racial differences in the use and outcome of neoadjuvant chemotherapy for breast cancer: results from the National Cancer Data Base. J Clin Oncol 33, 4267–4276.

Kim, S.J., Jung, K.H., Son, M.K., Park, J.H., Yan, H.H., Fang, Z., Kang, Y. W., Han, B., Lim, J.H., and Hong, S.S. (2017). Tumor vessel normalization by the PI3K inhibitor HS-173 enhances drug delivery. Cancer Lett 403, 339–353.

Kobayashi, N., Hikichi, M., Ushimado, K., Sugioka, A., Kiriyama, Y., Kuroda, M., and Utsumi, T. (2017). Differences in subtype distribution between screen-detected and symptomatic invasive breast cancer and their impact on survival. Clin Transl Oncol 19, 1232–1240.

Koo, H.R., Cho, N., Song, I.C., Kim, H., Chang, J.M., Yi, A., Yun, B.L., and Moon, W.K. (2012). Correlation of perfusion parameters on dynamic contrast-enhanced MRI with prognostic factors and subtypes of breast cancers. J Magn Reson Imag 36, 145–151.

Kutanzi, K.R., Yurchenko, O.V., Beland, F.A., Checkhun, V.'.F., and Pogribny, I.P. (2011). MicroRNA-mediated drug resistance in breast

cancer. Clin Epigenet 2, 171–185.
Li, L., Wang, K., Sun, X., Wang, K., Sun, Y., Zhang, G., and Shen, B. (2015). Parameters of dynamic contrast-enhanced MRI as imaging markers for angiogenesis and proliferation in human breast cancer. Med Sci Monit 21, 376–382.
Makris, A., Powles, T.J., Ashley, S.E., Chang, J., Hickish, T., Tidy, V.A., Nash, A.G., and Ford, H.T. (1998). A reduction in the requirements for mastectomy in a randomized trial of neoadjuvant chemoendocrine therapy in primary breast cancer. Ann Oncol 9, 1179–1184.
Makris, A., Powles, T.J., Kakolyris, S., Dowsett, M., Ashley, S.E., and Harris, A.L. (1999). Reduction in angiogenesis after neoadjuvant chemoendocrine therapy in patients with operable breast carcinoma. Cancer 85, 1996–2000.
McGuire, A., Casey, M.C., Waldron, R.M., Heneghan, H., Kalinina, O., Holian, E., McDermott, A., Lowery, A.J., Newell, J., Dwyer, R.M., et al. (2020). Prospective assessment of systemic microRNAs as markers of response to neoadjuvant chemotherapy in breast cancer. Cancers 12, 1820.
Murphy, B.L., Day, C.N., Hoskin, T.L., Habermann, E.B., and Boughey, J. C. (2018). Neoadjuvant chemotherapy use in breast cancer is greatest in excellent responders: triple-negative and HER2+ subtypes. Ann Surg Oncol 25, 2241–2248.
Pease, A.M., Riba, L.A., Gruner, R.A., Tung, N.M., and James, T.A. (2019). Oncotype DX® recurrence score as a predictor of response to neoadjuvant chemotherapy. Ann Surg Oncol 26, 366–371.
Pickles, M.D., Lowry, M., Manton, D.J., Gibbs, P., and Turnbull, L.W. (2005). Role of dynamic contrast enhanced MRI in monitoring early response of locally advanced breast cancer to neoadjuvant chemotherapy. Breast Cancer Res Treat 91, 1–10.
Prat, A., Galván, P., Jimenez, B., Buckingham, W., Jeiranian, H.A., Schaper, C., Vidal, M., Álvarez, M., Díaz, S., Ellis, C., et al. (2016). Prediction of response to neoadjuvant chemotherapy using core needle biopsy samples with the Prosigna assay. Clin Cancer Res 22, 560–566.
Rastogi, P., Anderson, S.J., Bear, H.D., Geyer, C.E., Kahlenberg, M.S., Robidoux, A., Margolese, R.G., Hoehn, J.L., Vogel, V.G., Dakhil, S.R., et al. (2008). Preoperative chemotherapy: updates of National Surgical Adjuvant Breast and Bowel Project Protocols B-18 and B-27. J Clin Oncol 26, 778–785.
Raychaudhuri, M., Bronger, H., Buchner, T., Kiechle, M., Weichert, W., and Avril, S. (2017). MicroRNAs miR-7 and miR-340 predict response to neoadjuvant chemotherapy in breast cancer. Breast Cancer Res Treat 162, 511–521.
Reis-Filho, J.S., and Pusztai, L. (2011). Gene expression profiling in breast cancer: classification, prognostication, and prediction. Lancet 378, 1812–1823.
Rouzier, R., Perou, C.M., Symmans, W.F., Ibrahim, N., Cristofanilli, M., Anderson, K., Hess, K.R., Stec, J., Ayers, M., Wagner, P., et al. (2005). Breast cancer molecular subtypes respond differently to preoperative chemotherapy. Clin Cancer Res 11, 5678–5685.
Saw, P.E., and Song, E.W. (2020). SiRNA therapeutics: a clinical reality. Sci China Life Sci 63, 485–500.
Saw, P.E., Xu, X., Chen, J., and Song, E.W. (2021). Non-coding RNAs: the new central dogma of cancer biology. Sci China Life Sci 64, 22–50.
Sparano, J.A., Crager, M.R., Tang, G., Gray, R.J., Stemmer, S.M., and Shak, S. (2021). Development and validation of a tool integrating the 21-gene recurrence score and clinical-pathological features to individualize prognosis and prediction of chemotherapy benefit in early breast cancer. J Clin Oncol 39, 557–564.
Tan, W., Luo, W., Jia, W., Liang, G., Xie, X., Zheng, W., Song, E., Su, F., and Gong, C. (2016). A combination of nottingham prognostic index and IHC4 score predicts pathological complete response of neoadjuvant chemotherapy in estrogen receptor positive breast cancer. Oncotarget 7, 87312–87322.
Tang, H., Song, C., Ye, F., Gao, G., Ou, X., Zhang, L., Xie, X., and Xie, X. (2019). miR-200c suppresses stemness and increases cellular sensitivity to trastuzumab in HER2+ breast cancer. J Cell Mol Med 23, 8114–8127.
Viallard, C., and Larrivée, B. (2017). Tumor angiogenesis and vascular normalization: alternative therapeutic targets. Angiogenesis 20, 409–426.
Vickers, A.J., Cronin, A.M., Elkin, E.B., and Gonen, M. (2008). Extensions to decision curve analysis, a novel method for evaluating diagnostic tests, prediction models and molecular markers. BMC Med Inform Decis Mak 8, 53.
Vincent-Salomon, A., Rousseau, A., Jouve, M., Beuzeboc, P., Sigal-Zafrani, B., Fréneaux, P., Rosty, C., Nos, C., Campana, F., Klijanienko, J., et al. (2004). Proliferation markers predictive of the pathological response and disease outcome of patients with breast carcinomas treated by anthracycline-based preoperative chemotherapy. Eur J Cancer 40, 1502–1508.
von Minckwitz, G., Untch, M., Nüesch, E., Loibl, S., Kaufmann, M., Kümmel, S., Fasching, P.A., Eiermann, W., Blohmer, J.U., Costa, S.D., et al. (2011). Impact of treatment characteristics on response of different breast cancer phenotypes: pooled analysis of the german neo-adjuvant chemotherapy trials. Breast Cancer Res Treat 125, 145–156.
von Minckwitz, G., Untch, M., Blohmer, J.U., Costa, S.D., Eidtmann, H., Fasching, P.A., Gerber, B., Eiermann, W., Hilfrich, J., Huober, J., et al. (2012). Definition and impact of pathologic complete response on prognosis after neoadjuvant chemotherapy in various intrinsic breast cancer subtypes. J Clin Oncol 30, 1796–1804.
von Minckwitz, G., Huang, C.S., Mano, M.S., Loibl, S., Mamounas, E.P., Untch, M., Wolmark, N., Rastogi, P., Schneeweiss, A., Redondo, A., et al. (2019). Trastuzumab emtansine for residual invasive HER2-positive breast cancer. N Engl J Med 380, 617–628.
Whitworth, P., Stork-Sloots, L., de Snoo, F.A., Richards, P., Rotkis, M., Beatty, J., Mislowsky, A., Pellicane, J.V., Nguyen, B., Lee, L., et al. (2014). Chemosensitivity predicted by blueprint 80-gene functional subtype and MammaPrint in the Prospective Neoadjuvant Breast Registry Symphony Trial (NBRST). Ann Surg Oncol 21, 3261–3267.
Yee, D., Demichele, A., Isaacs, C., Symmans, F., Yau, C., Albain, K.S., Hylton, N.M., Forero-Torres, A., Van't Veer, L.J., Perlmutter, J., et al. (2018). Pathological complete response predicts event-free and distant disease-free survival in the I-SPY2 TRIAL. Cancer Res 78, GS3-08-GS3-08.
Yi, B., Kang, D.K., Yoon, D., Jung, Y.S., Kim, K.S., Yim, H., and Kim, T. H. (2014). Is there any correlation between model-based perfusion parameters and model-free parameters of time-signal intensity curve on dynamic contrast enhanced MRI in breast cancer patients? Eur Radiol 24, 1089–1096.
Yu, F., Deng, H., Yao, H., Liu, Q., Su, F., and Song, E. (2010). MiR-30 reduction maintains self-renewal and inhibits apoptosis in breast tumor-initiating cells. Oncogene 29, 4194–4204.
Zhao, Z., Xiao, X., Saw, P.E., Wu, W., Huang, H., Chen, J., and Nie, Y. (2020). Chimeric antigen receptor T cells in solid tumors: a war against the tumor microenvironment. Sci China Life Sci 63, 180–205.

SUPPORTING INFORMATION

The supporting information is available online at https://doi.org/10.1007/s11427-022-2104-3. The supporting materials are published as submitted, without typesetting or editing. The responsibility for scientific accuracy and content remains entirely with the authors.